Supporting Information

Stable carbon-encapsulated nano zero-valent cobalt catalyst for ultrafast elimination of emerging contaminants in water

Fengming Situ[a, 1], Chengzhen Meng[a, 1], Zhihui Yin[a], Peng Zhang[a], Shuaiqi Zhang[a], Jiaxin Ou[a], Ziting Ma[a], Chun Hu[a], Ning Jiang[b, *], and Fan Li[a, *]

[a]Key Laboratory for Water Quality and Conservation of the Pearl River Delta, Ministry of Education, Institute of Environmental Research at Greater Bay, Guangzhou University, Guangzhou, 510006, China

[b]State Key Laboratory of Environmental Criteria and Risk Assessment, Chinese Research Academy of Environmental Sciences, Beijing 100012, China

[1]These authors contributed equally to this work.

*Corresponding author

Ning Jiang, E-mail: jiangning@craes.org.cn, ORCID ID: 0009-0000-3561-0499

Fan Li, E-mail: lifan@gzhu.edu.cn, ORCID ID: 0000-0001-5801-127X

Text S1. Chemicals and materials.

Cobalt chloride ($CoCl_2$, 98.0%), 2,2-Bis (4-Hydroxyphenol) Propane ($C_{15}H_{16}O_2$, BPA, 98.0%), Sulfamethoxazole ($C_{10}H_{11}N_3O_3S$, SMZ, 98.0%), 2,4-dichlorophenol ($C_6H_4Cl_2O$, 2,4-DCP, 98.0%), (methylsulfinyl) benzene (C_7H_8OS, PMSO, 98.0%), methyl phenyl sulfone ($C_7H_8O_2S$, $PMSO_2$, 98.0%), 2,2,6,6-tetramethyl-4-piperidinol ($C_9H_{19}NO$, TEMP, 98.0%), sodium sulfate (Na_2SO_4, 99.0%), potassium monopersulfate triple salt ($K_5/2H_3/2S_2O_9$, PMS, 42.8–46.0%), rhodamine B ($C_{28}H_{31}ClN_2O_3$, RhB, 96.0%), humic acid (HA, 90.0%), nafion perfluorinated resin ($C_9HF_{17}O_5S$), and *p*-benzoquinone ($C_6H_4O_2$, *p*-BQ, 99.0%) were obtained from Adamas-beta Co., Ltd. Sodium thiosulfate ($Na_2S_2O_3$, 99.0%), furfuryl alcohol ($C_5H_6O_2$, FFA, 98.0%), Ciprofloxacin ($C_{17}H_{18}FN_3O_3$, CIP, 98.0%), Sodium bicarbonate ($NaHCO_3$, 99.8%) and tert-butanol ($C_4H_{10}O$, TBA, 99.0%) were obtained from Shanghai Macklin Biochemical Co., Ltd. Ethanol (CH_3CH_2OH, EtOH, 99.7%), Methanol (CH_3OH, MeOH, 99.7%), sodium dihydrogenorthophosphate (NaH_2PO_4, 99.0%) and sodium chloride (NaCl, 99.5%) were obtained from General-Reagent® Co., Ltd. 5,5-dimethyl-1-pyrroline *N*-oxide ($C_6H_{11}NO$, DMPO) was purchased from DOJINDO, Japan. Tetracycline ($C_{22}H_{24}N_2O_8$, TC, 91.0%) was obtained from J&K Science Co., Ltd. Phenol solution (C_6H_6O, 99.5%) was obtained from Shanghai Meryer Co., Ltd. Melamine (C_3H_6N6, 99.0%) was obtained from Sinopharm Chemical Reagent Co., Ltd. sodium nitrate ($NaNO_3$, AR) were obtained from Guangdong Guangshi Regent Technology Co., Ltd. All solutions were prepared using ultrapure water (Milli-Q, 18.2 MΩ cm) produced from a purification system.

Text S2. The determination of Co contents in nZVCo@NC.

The procedure for determining the Co content in the nZVCo@NC catalysts as follows: A 2.0 mg portion of the nZVCo@NC catalyst was placed in a Teflon crucible, followed by the addition of 3.0 mL sulfuric acid and 2.0 mL nitric acid. The resulting suspension was heated on an electric hot plate at 200 ℃ until it turned clear and transparent. After being cooled to room temperature, the solution was transferred to a 50.0 mL volumetric flask, diluted with water to the calibration mark, and shaken thoroughly. Finally, a 5.0 mL aliquot of the solution was taken, and the concentrations of Co were measured using inductively coupled plasma optical emission spectrometry (ICP-OES). The Co content in the nZVCo@NC catalyst was calculated using Equation S1.

$$Ratio_M = \frac{c \times 0.05L}{2\ mg} \times 100\ wt\% \qquad \text{(S1)}$$

Where c and $Ratio_M$ are the metal concentration (mg L^{-1}) measured by ICP-OES and metal content in the nZVCo@NC catalysts.

Text S3. Calculation of the modified rate constant.

The pseudo-first-order kinetic constant (k_{obs}) is determined by equation S2

$$\ln\left(\frac{C_t}{C_0}\right) = -k_{obs} \times t \quad \text{(S2)}$$

where C_t and C_0 are the pollutant concentration at reaction time (t) and initial moment, respectively.

The modified rate constant (k_m) is calculated as equation S3

$$k_m = \frac{k_{obs} \times [P]}{[cat] \times [PMS]} \quad \text{(S3)}$$

Where k_{obs} = pseudo-first-order kinetic constant, [P] = Concentration of pollutants, [cat] = catalyst dosage, and [PMS] = PMS concentration.

Text S4. Details of the DMPO- and TEMP-trapping EPR analysis.

The reaction was performed in a beaker with stirring via a magnetic stirrer. The first and second sampling times were set at 15 seconds and 45 seconds after the initiation of the reaction, respectively. At each time point, 1.0 mL of the reaction mixture was taken, and 20 μL of DMPO/TEMP (5.0 M) was added thereto. The resulting suspension was then transferred into a micropipette and loaded into an EPR quartz tube for the detection of $SO_4^{\bullet-}$, •OH, $O_2^{\bullet-}$, and $^1O_2$. The reaction conditions were as follows: catalyst dosage = 0.06 g L^{-1}, $[PMS]_0$ = 0.50 mM, $[2,4\text{-DCP}]_0$ = 50 μM, and temperature = 25 ℃.

Text S5. Details of the in situ Raman analysis.

The activation reaction of PMS was conducted in a beaker under magnetic stirring. At predetermined time intervals, 50 μL of the suspension mixture was sampled. The conversion of HSO^{5-} to SO_4^{2-} was measured utilizing a 532 nm laser. The reaction parameters were as follows: catalyst dosage = 0.2 g L^{-1}, initial PMS concentration $[PMS]_0$ = 0.50 M, initial 2,4-DCP concentration $[2,4\text{-DCP}]_0$ = 500 μM, and temperature = 25 ℃.

Text S6. Details of electrochemical test.

The electrochemical properties of catalysts were evaluated using a Zahner electrochemical workstation (Zahner Zennium Pro) in a standard three-electrode configuration. In this setup, an Ag/AgCl electrode served as the reference electrode, a platinum sheet functioned as the counter electrode, and 50 mL of 0.1 M Na_2SO_4 solution was used as the electrolyte. A 500 μL mixture of catalyst solution (10 g L^{-1}) and Nafion solution (20 wt%) was deposited onto a 1×1 cm^2 indium-tin-oxide (ITO) conductive glass electrode, which acted as the working electrode. Using the chronoamperometry technique, PMS and 2,4-DCP were sequentially introduced into the reaction system, with the resulting current variations recorded throughout the process.

Text S7. Details of galvanic oxidation process (GOP) system.

A galvanic oxidation process (GOP) system was developed to separate PMS and 2,4-DCP into two half-cells to verify the electron transfer process in PMS activation and 2,4-DCP decomposition. The same working electrode preparation method employed in the electrochemical experiments was utilized (Text S6), except that graphite electrodes were utilized in lieu of platinum electrodes. A KCl agar salt bridge and an ammeter connected the two half-cells to maintain electrical neutrality and record current changes during the reaction. The reaction solutions used were all prepared with 0.1 M Na_2SO_4 solution. The reaction solutions (50 mL) were placed in each of the two half-cells in advance, and the opening of the ammeter was taken to mark the commencement of the reaction, with the subsequent recording of the change in current in the system at different times.

Text S8. Details of theoretical calculations

The DFT calculations were carried out using DMol^3 module [1,2]. Exchange and correlation effects were treated within the generalized gradient approximation (GGA) using the Perdew-Burke-Ernzerhof (PBE) functional [3]. The all-electron relativistic (AER) function combined with the double numerical plus polarization (DNP) basis set was adopted to describe the interactions between atomic nuclei and electrons [1,4]. The convergence criteria for electronic energy and geometric optimization were set as 2×10^{-5} Ha and a maximum force of 0.004 Ha/Å. To avoid spurious interactions between periodic images, a vacuum layer of 15 Å was applied. The van der Waals (vdW) interaction were incorporated using the Grimme dispersion correction scheme [5]. Solvation effects were considered via the conductor-like screening model (COSMO) with a dielectric constant of 78.54 to simulate the water environment [6]. The adsorption energy (E_{ads}) was defined as $E_{ads}=E_{sys}-E_{cat}-E_{mol}$, where E_{sys}, E_{cat} and E_{mol} represent the total energies of the adsorption system, the catalyst, and the adsorbate molecule, respectively.

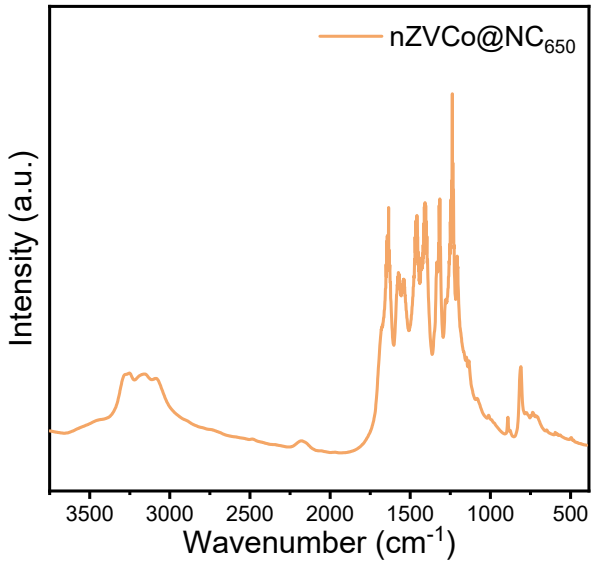

Fig. S1. FTIR spectrum of nZVCo@NC_{650}.

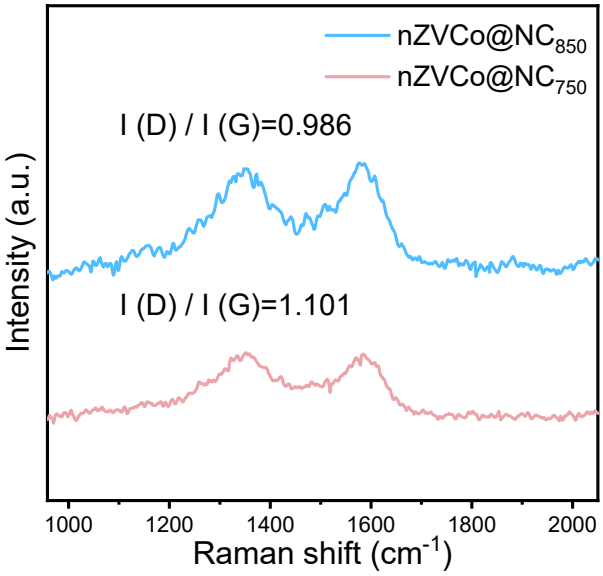

Fig. S2. Raman spectra of nZVCo@NC_{750} and nZVCo@NC_{850}.

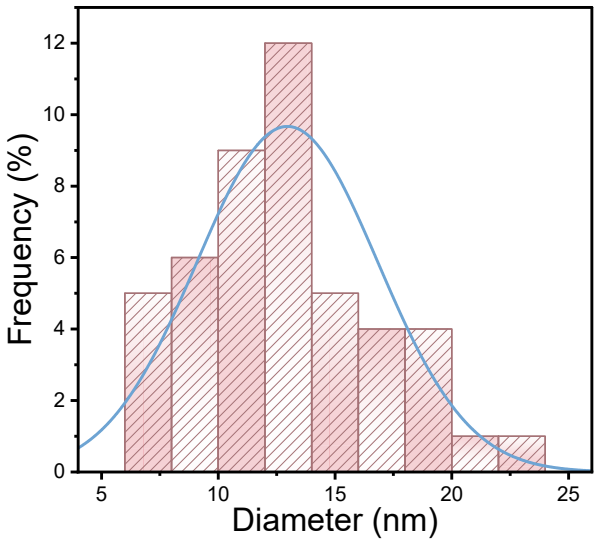

Fig. S3. Statistical analysis of the particle size distribution of nZVCo@NC

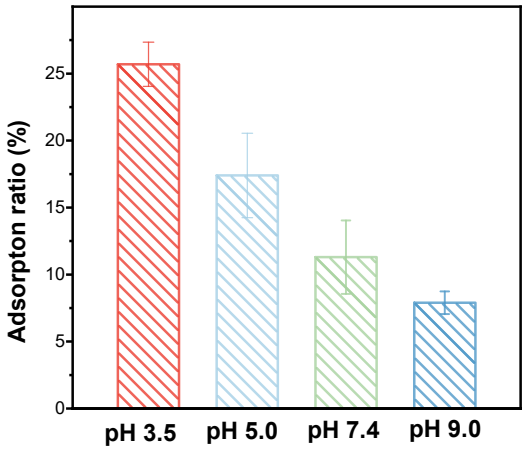

Fig. S4. Effect of pH on adsorption capacity.

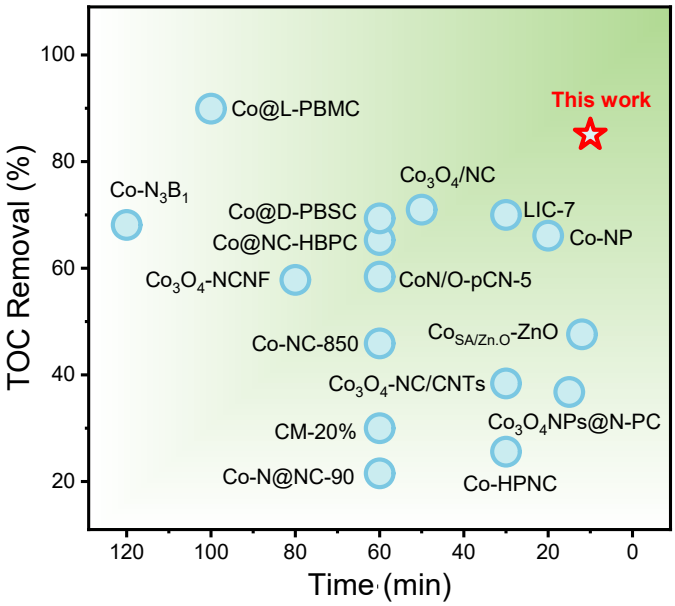

Fig. S5 comparison of the TOC removal rate

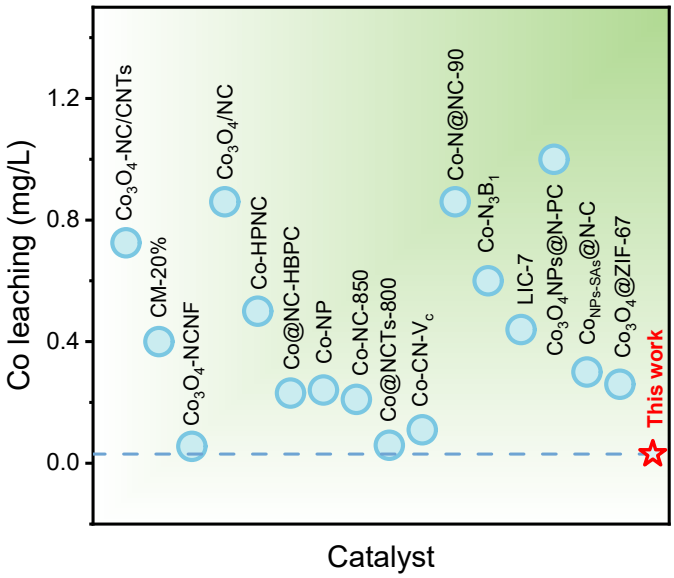

Fig. S6 comparison of the cobalt ion leaching concentrations

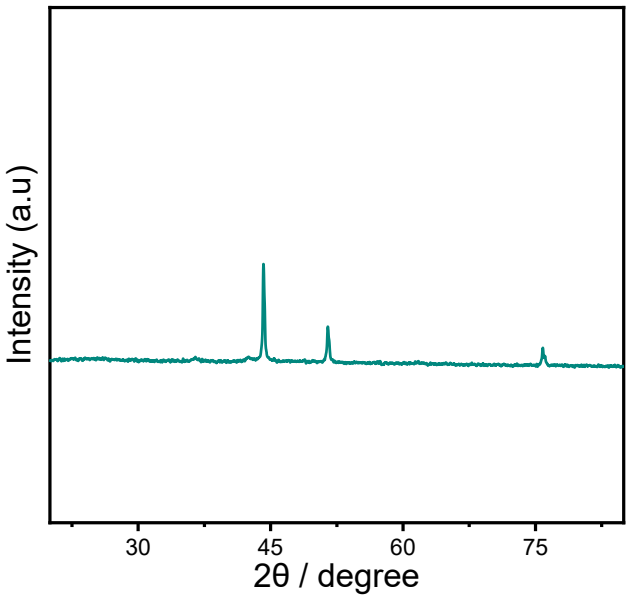

Fig. S7. XRD pattern of used nZVCo@NC.

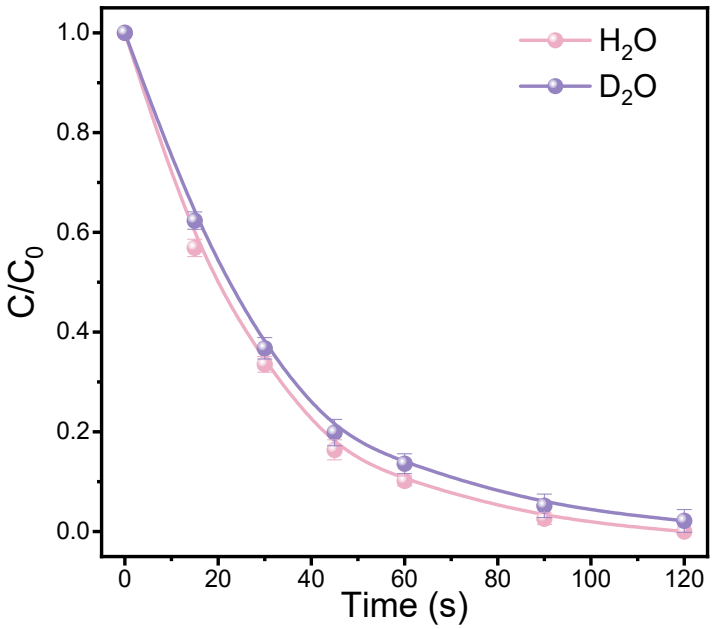

Fig. S8. Effect of D_2O on 2,4-DCP degradation in nZVCo@NC + PMS system.

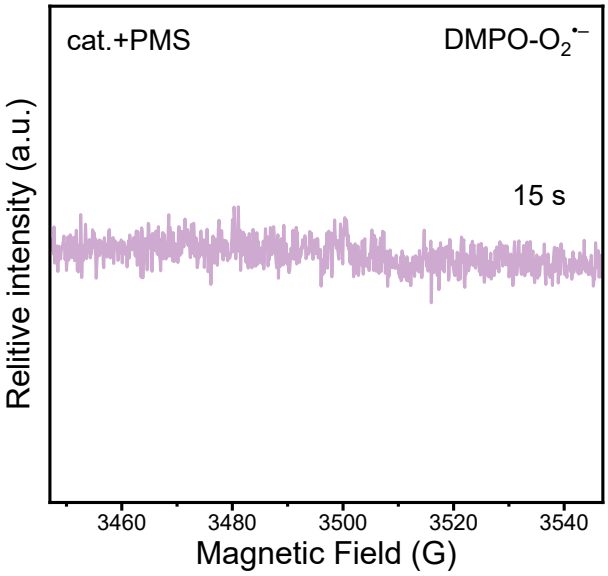

Fig. S9. EPR spectrum using DMPO as the trapping agent in methanol.

Table S1. Molecular structures of organic compounds, along with operational parameters of HPLC and UV-vis spectrophotometer.

Compound	Structure	Detection Wavelength (nm)	Mobile Phase (V/V)
tetracycline (TC)	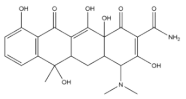	355	Methanol : water (0.8% phosphoric acid): acetonitrile = 20:60:20
bisphenol A (BPA)	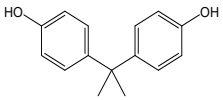	225	Methanol : water = 70:30
Ciprofloxacin (CIP)	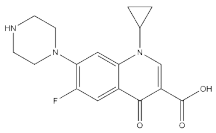	278	water (0.8% phosphoric acid): acetonitrile = 80:20
sulfamethoxazole （SMZ）	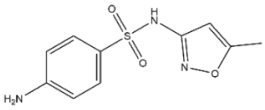	266	Methanol : water = 55:45
Phenol	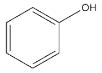	270	Methanol : water = 60:40
2,4-dichlorophenol (2,4-DCP)	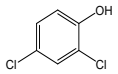	282	Methanol : water = 80:20
methyl phenyl sulfoxide (PMSO)	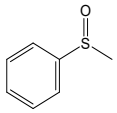	218	Acetonitrile : water (0.8% phosphoric acid) = 40:60
methyl phenyl sulfone ($PMSO_2$)	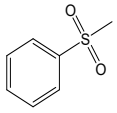	218	Acetonitrile : water (0.8% phosphoric acid) = 40:60
Rhodamine B (RhB)	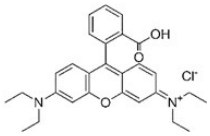	552	/

Table S2. Comparison of the normalized rate constants of pollutant degradation by PMS activation with the previously reported catalysts. The normalized rate constant (k_m) model was obtained after multiplying the pseudo-first-order kinetic constants (k_{obs}) by the pollutant concentration and dividing by the catalyst and PMS dosage.

Catalyst ($g\ L^{-1}$)	PMS (mM)	Pollutant ($mg\ L^{-1}$)	k_{obs} (min^{-1})	k_m ($min^{-1}M^{-1}$)	Ref.
nZVCo@NC(0.06)	0.50	2,4-DCP (8.15)	2.3260	631.897	This work
BC (0.1)	1.30	TC (40)	0.00064	0.197	7
CNTs (0.04)	0.50	2,4-DCP (16.3)	0.0259	21.100	8
pCN (0.2)	0.65	TC (20)	0.0020	0.302	9
CN (0.3)	1.25	Phenol (50)	0.0052	0.687	10
B-CN (0.2)	2.00	TC (50)	0.0184	2.300	11
O-CN (0.4)	0.80	SMX (5)	0.0117	0.183	12
Co_3O_4 (0.2)	0.65	Phenol (20)	0.029	4.460	13
Co_3O_4/BC (0.1)	1.30	TC (40)	0.2510	77.230	7
Co_3O_4-NC/CNTs (0.04)	0.50	2,4-DCP (16.3)	0.1395	113.690	8
CM-20% (0.1)	0.98	BPA (20)	0.3984	81.310	14
CoN/O-pCN-5 (0.2)	0.65	TC (20)	0.0676	10.390	9
Co_3O_4/NC (0.05)	1.00	TCH (20)	0.0980	39.200	15
Co_3O_4NPs@N-PC (0.2)	0.25	SMZ (12.7)	0.7700	195.580	16
Co-HPNC (0.05)	1.00	AO7 (35.032)	0.4319	302.610	17
Co@L-PBMC (0.1)	0.50	TC (20)	0.1590	63.600	18
Co@NC-HBPC (0.2)	0.50	NTP (50)	0.1230	61.500	19
Co-NP (0.1)	2.00	CBP (20)	0.1846	18.460	20
Co-NC-850 (0.025)	0.80	RhB (80)	0.1480	592.000	21
Co@NCTs-800 (0.05)	1.30	TC (30)	0.0664	30.660	22
$Co_{NPs\text{-}SAs}$@N-C (0.12)	1.60	SDZ (20)	0.0412	4.2920	23
$Co_3(HITP)_2$ (20)	0.16	CBZ (5)	1.4700	2.268	24

Co-CN-V_c (0.3)	1.25	Phenol (50)	1.0200	136.00	[10]
CoSAC@MT (0.5)	0.50	SMX (10)	0.2330	9.320	[25]
$Co_{SA/Zn.O}$-ZnO (0.1)	0.50	SMX (10)	0.4910	98.200	[26]
Co-N_3B_1 (0.2)	2.00	TC (50)	1.3373	167.163	[11]
LIC-7 (0.08)	0.49	Phenol (20)	0.6880	351.020	[27]

Table S3. Comparison of the TOC removal rate with the previously reported catalysts.

Catalyst	Time (min)	TOC removal (%)	Ref.
Co_3O_4-NC/CNTs	30	38.4	[8]
CM-20%	60	30	[14]
CoN/O-pCN-5	60	58.42	[9]
Co_3O_4/NC	50	71	[15]
Co-HPNC	30	25.6	[17]
Co@L-PBMC	100	89.94	[18]
Co@NC-HBPC	60	65.3	[19]
Co-NP	20	66.11	[20]
Co-NC-850	60	45.9	[21]
$Co_{SA/Zn.O}$-ZnO	12	47.6	[26]
Co-N_3B_1	120	68.12	[11]
LIC-7	30	70	[27]
Co_3O_4NPs@N-PC	15	36.8	[16]
Co_3O_4-NCNF	80	57.8	[28]
Co@D-PBSC	60	69.34	[29]
Co-N@NC-90	60	21.53	[30]

Table S4. Comparison of the cobalt ion leaching concentrations with the previously reported catalysts.

Catalyst	Co leaching (mg/L)	Ref.
Co_3O_4-NC/CNTs	0.725	8
CM-20%	0.400	14
Co_3O_4-NCNF	0.056	28
Co_3O_4/NC	0.860	15
Co-HPNC	0.500	17
Co@NC-HBPC	0.231	19
Co-NP	0.241	20
Co-NC-850	0.210	21
Co@NCTs-800	0.059	22
Co-CN-V_c	0.110	10
Co-N@NC-90	0.860	30
Co-N_3B_1	0.600	11
LIC-7	0.440	27
Co_3O_4NPs@N-PC	1.000	16
$Co_{NPs-SAs}$@N-C	0.300	23
Co_3O_4@ZIF-67	0.260	31

References

1 B. Delley, An All-Electron Numerical Method for Solving the Local Density Functional for Polyatomic Molecules. *J. Chem. Phys.*, 1990, **92**, 508–517.

2 B. Delley, From Molecules to Solids with the DMol^2 Approach. *J. Chem. Phys.*, 2000, **113**, 7756–7764.

3 J. P. Perdew, K. Burke and M. Ernzerhof, Generalized Gradient Approximation Made Simple. *Phys. Rev. Lett.*, 1996, **77**, 3865–3868.

4 D. D. Koelling and B. N. Harmon, A Technique for Relativistic Spin-Polarised Calculations. *J. Phys. C: Solid State Phys.*, 1977, **10**, 3107–3114.

5 S. Grimme, Semiempirical GGA-type density functional constructed with a long-range dispersion correction. *J. Comput. Chem.*, 2006, **27**, 1787–1799.

6 B. Delley, The Conductor-like Screening Model for Polymers and Surfaces. *Mol. Simul.*, 2006, **32**, 117–123.

7 M. Xiong, J. Yan, G. Fan, Y. Liu, B. Chai, C. Wang and G. Song, Built-in Electric Field Mediated Peroxymonosulfate Activation over Biochar Supported-Co_3O_4 Catalyst for Tetracycline Hydrochloride Degradation. *Chem. Eng. J.*, 2022, **444**, 136589.

8 H. Wang, D. Wang, C. Sun, X. Zhao, C. Xu, Z. Li, Y. Hou, L. Lei, B. Yang and X. Duan, Oriented Generation of $^1O_2$ from Peroxymonosulfate via Co_3O_4 Facet Engineering. *Appl. Catal. B Environ. Appl. Catal. B Environ.*, 2025, **364**, 124854.

9 X. Liu, D. Huang, C. Lai, L. Qin, S. Liu, M. Zhang and Y. Fu, Single Cobalt Atom Anchored on Carbon Nitride with Cobalt Nitrogen/Oxygen Active Sites for Efficient Fenton-like Catalysis. *J. colloid Interface Sci.*, 2023, **629**, 417–427.

10 F. Miao, C. Wang, T. Cheng, Y. Liu, R. Wang, X. Duan and W. Jiao, Carbon Vacancy Engineering Regulates the Cobalt-Single-Atom Site for Co(IV)=O Efficient Generation and Its Ultrafast Degradation of Electron-Rich Pollutants. *Water Res.*, 2026, **289**, 124998.

11 W. Li, X. Cai, X. Zhou, Z. Luo, C. Yan, J. Ge, Z. Huang, Y. Zhang, P. Wang, Y. Luo and J. Deng, Morphology-Coordination Dual Engineering in Cobalt Single-Atom Catalysts: Steering Peroxymonosulfate Activation into Selective $^1O_2$ Generation for Efficient Antibiotic Degradation. *Appl. Catal. B Environ.*, 2026, **382**, 125933.

12 H. Zhang, Y. Zhao, H. Li, J. Wang and Y. Yu, Photocatalytic Activation of Peroxymonosulfate by Oxygen Doped Graphitic C_3N_4 with Oxygen Vacancy for Drug Degradation: Theoretical Calculation and Recyclable Products. *J. Environ. Chem. Eng.*, 2025, **13**, 115318.

13 H. Zhang, Q. An, Y. Su, X. Quan and S. Chen, Co_3O_4 with Upshifted d-Band Center and Enlarged Specific Surface Area by Single-Atom Zr Doping for Enhanced PMS Activation. *J. Hazard. Mater.*, 2023, **448**, 130987.

14 Y. Liu, R. Luo, Y. Li, J. Qi, C. Wang, J. Li, X. Sun and L. Wang, Sandwich-like Co_3O_4/MXene Composite with Enhanced Catalytic Performance for Bisphenol A Degradation. *Chem. Eng. J.*, 2018, **347**, 731–740.

15 Q. Li, Z. Ren, Y. Liu, C. Zhang, J. Liu, R. Zhou, Y. Bu, F. Mao and H. Wu, Petal-like Hierarchical Co_3O_4/N-Doped Porous Carbon Derived from Co-MOF for Enhanced Peroxymonosulfate Activation to Remove Tetracycline Hydrochloride. *Chem. Eng. J.*, 2023, **452**, 139545.

16 H. Mohtasham, M. Rostami, B. Gholipour, A. M. Sorouri, H. Ehrlich, M. R. Ganjali, S. Rostamnia, M. Rahimi-Nasrabadi, A. Salimi and R. Luque, Nano-Architecture of MOF (ZIF-

67)-Based Co_3O_4 NPs@N-Doped Porous Carbon Polyhedral Nanocomposites for Oxidative Degradation of Antibiotic Sulfamethoxazole from Wastewater. *Chemosphere*, 2023, **310**, 136625.

17 Y. Long, S. Li, P. Yang, X. Chen, W. Liu, X. Zhan, C. Xue, D. Liu and W. Huang, Synthesis of ZIF-67 Derived Honeycomb Porous Co/NC Catalyst for AO7 Degradation via Activation of Peroxymonosulfate. *Sep. Purif. Technol.*, 2022, **286**, 120470.

18 Y. Wang, D. Li, X. Ge, J. Yu, Y. Zhao and Y. Bu, Anchored Cobalt Nanoparticles on Layered Perovskites for Rapid Peroxymonosulfate Activation in Antibiotic Degradation. *Adv. Mater.*, 2024, **36**, 2402935.

19 Y. Liu, H. Zhou, Z. Shi, W. Zhang, C. Jin, L. Zhu, C. Tang, G. Liu, S. Huo and Z. Kong, Interfacial-Engineered MOFs-POPs Derived Co@N-Doped Carbon Catalyst in Boosting Peroxymonosulfate Activation and Pollutant Degradation: Roles of Microstructure and Exposed Facets. *Carbon*, 2024, **218**, 118779.

20 Q. Bi, Y. Zhang, C. Zhang, K. Wang, S. Zhao and J. Xue, Precise Control of Cobalt Active Site Size to Switch ROS Pathways: Millimeter-Scale Carbon Beads Derived from Dual MOFs for Targeted Degradation of Drug Pollutants. *Appl. Catal. B Environ.*, 2026, **383**, 126046.

21 X. Chen, J. Zhou, H. Yang, H. Wang, H. Li, S. Wu and W. Yang, PMS Activation by Magnetic Cobalt-N-Doped Carbon Composite for Ultra-Efficient Degradation of Refractory Organic Pollutant: Mechanisms and Identification of Intermediates. *Chemosphere*, 2022, **287**, 132074.

22 Y. Lu, Y.-K. Li, C. Huang, R. Chen, Y. Chen and C. Wang, Autocatalytic Formed Bamboo-like N-Doped Carbon Nanotubes Encapsulated with Co Nanoparticles as Highly Efficient Catalyst for Activation of Peroxymonosulfate toward Degradation of Tetracycline. *React. Funct. Polym.*, 2023, **183**, 105482.

23 Y. Hu, H. Guo, Y. Lv, C. Tian, Y. Lin and H. Liu, Axial Enhancement on Non-Radicals Generation in PMS Activation Process Mediated with Co Single-Atom Catalyst Encapsulated Nanoparticles. *J. Hazard. Mater.*, 2025, **496**, 139513.

24 M. Li, D. Xia, W. Zhang, F. Sun, G. Zhang, L. Lin, Z. Gong, B. Li and X. Li, Facile Synthesis of High Loading and Highly Electron-Delocalized Co Single-Atom Catalyst for PMS Activation: An in-Depth Study of Molecular Orbital and Catalytic Mechanisms. *J. Hazard. Mater.*, 2025, **499**, 140298.

25 K. Yin, Y. Tang, Z. Li, H. Zhao, X. Xu, Q. Li, Q. Yue, Y. Gao and B. Gao, Powerful Fenton-like Reactions Derived from Montmorillonite Modulated Co Single Atom: Key Role of Heterogeneous High-Valent Co (IV)-Oxo. *Water Res.*, 2025, **285**, 124130.

26 Z.-Q. Zhang, P.-J. Duan, J.-X. Zheng, Y.-Q. Xie, C.-W. Bai, Y.-J. Sun, X.-J. Chen, F. Chen and H.-Q. Yu, Nano-Island-Encapsulated Cobalt Single-Atom Catalysts for Breaking Activity-Stability Trade-off in Fenton-like Reactions. *Nat. Commun.*, 2025, **16**, 115.

27 H. Zou, H. Wang, H. Sun, W. Sun, S. Luo, T. Li, X. Duan and S. Zhan, Single-Atom Cobalt Catalysts Encapsulating Cobalt Nanoparticles with Built-In Electric Field for Ultrafast and Lasting Peroxymonosulfate Activation. *ACS EST Water*, 2024, **4**, 2433–2444.

28 G. Yi, M. Ye, J. Wu, Y. Wang, Y. Long and G. Fan, Facile Chemical Blowing Synthesis of Interconnected N-Doped Carbon Nanosheets Coupled with Co_3O_4 Nanoparticles as Superior Peroxymonosulfate Activators for p-Nitrophenol Destruction: Mechanisms and Degradation Pathways. *Appl. Surf. Sci.*, 2022, **593**, 153244.

29 C. Zhao, L. Xu, Y. Wang, H. Qiao, Y. Zhao, D. Li and Y. Bu, Accelerated Peroxymonosulfate

Activation over Defective Perovskite with Anchored Cobalt Nanoparticles for Organic Contaminant Removal. *Chem. Eng. J.*, 2024, **496**, 153712.

30 H. Liu, Z. He, J. Li and S. Zhao, Well-Dispersed Cobalt Nanoparticles Encapsulated on ZIF-8-Derived *N*-Doped Porous Carbon as an Excellent Peroxymonosulfate Activator for Sulfamethoxazole Degradation. *Chem. Eng. J.*, 2023, **451**, 138597.

31 M. Dong, G. Zhang and G. Ma, Co_3O_4@ZIF-67 Core–Shell Heterogeneous Catalyst for Degradation of Dye Contaminants. *Inorg. Chem. Commun.*, 2023, **158**, 111418.